

Fig. 3 Reynolds number vs  $H\delta r_0^{5/2}\delta p$  for varying values of  $\delta p$ ,  $\delta r_0$ ,  $\xi$ , and  $H$ .

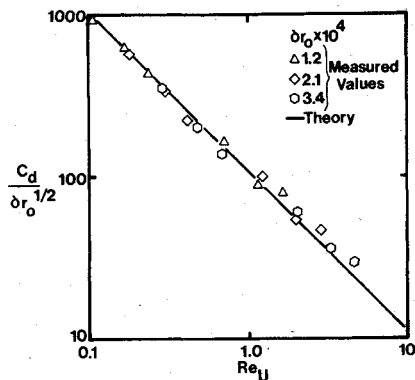


Fig. 4  $C_d/\delta r_0^{1/2}$  vs the Reynolds number for a centered piston-sphere configuration.

axial direction. This fact combined with an integral continuity condition

$$\int_0^{2\pi} \int_{r_i-\Delta r}^{r_i} u_x r dr d\theta = q \quad (5)$$

yields a system of differential equations describing the flowfield. Equations (1) and (5) are solved for the volumetric flow rate  $q$  with an imposed pressure differential  $\Delta p$  and/or piston motion  $U$ . The viscous drag can then be derived and is

$$F_x = - \int_{-\infty}^{\infty} \int_0^{2\pi} \mu (\partial u_x / \partial r)_{r=r_i-\Delta r} (r_i - \Delta r) d\theta dx \quad (6)$$

where  $F_x$  denotes the axial viscous force.

Equations (1), (5) and (6) can be integrated provided  $\Delta r$  and the appropriate boundary conditions, i.e.,  $r=r_i$ ,  $u_x=0$ ,  $r=r_i-\Delta r$ ,  $u_x=U$  are specified. The pressure gradient term can be linked to the volumetric flow rate via the integral continuity condition and

$$\frac{H\delta p \delta r_0^{5/2}}{\pi} = \frac{8Re}{\sqrt{2}\xi^2} \left[ 1 - \frac{(1 + [1 + 3/2\xi^2]^{1/2})^{1/2}}{(2 + 3\xi^2)^{1/2}} \right] - \frac{3Re_U}{(1 + 3/2\xi^2)^{1/2} [1 + (1 + 3/2\xi^2)^{1/2}]^{1/2}} \quad (7)$$

A similar relationship can be obtained for viscous and/or frictional force and

$$\frac{Re_U^2 C_d}{\pi \delta r_0^{1/2}} = \frac{12Re_U [1 + (1 + 3/2\xi^2)^{1/2}]^{1/2}}{(1 + 3/2\xi^2)^{1/2}} - \frac{24Re}{(1 + 3/2\xi^2)^{1/2} [1 + (1 + 3/2\xi^2)^{1/2}]^{1/2}} \quad (8)$$

Note that  $Re = q\rho/\pi r_i \mu$ ,  $Re_U = 2r_i \delta r_0 \rho U/\mu$ ,  $\delta r_0 = \Delta r_0/r_i$ ,  $\xi = e/\Delta r_0$ ,  $\delta p = \Delta p/p_r$ ,  $C_d = F_x/\pi r_i^2 \rho U^2$ ,  $H = r_i^2 \rho p_r/\mu^2$ , where  $\rho$  denotes the fluid density, and  $p_r$  a reference pressure.

### Comparison of Theoretical and Experimental Results

The results of the Poiseuille flow experiments are shown in Fig. 3. The theoretical relationship is also shown indicating that Eq. (7) is sufficient to correlate the data over a wide range of operating conditions. The deviation between predicted and measured results is greater with increased Reynolds number. This deviation is generally attributed to inertia effects<sup>1,5</sup> and/or variation in fluid properties.

The Couette flow experimental apparatus, Fig. 2, was used to determine drag coefficient values. These data are plotted in Fig. 4 and are compared to the theoretical values of Eq. (8). This relationship was maintained throughout the range of test conditions implying the existence of a lubricating film between the piston and cylinder for all configurations. Again the theoretical and experimental results tend to diverge at larger  $Re_U$  values which is probably due to inertia effects.

### Summary

Experimental investigations were carried out demonstrating the feasibility of using spherical pistons in right circular cylinders having very small clearances. A lubricating film was maintained in the most severe cases with piston-cylinder friction at acceptable levels. An analytic model was derived for this flow case using the assumptions of low Reynolds number and very small clearances. The experimental and theoretical results were in general agreement through the range of values appropriate for practical applications of the device.

### References

- <sup>1</sup>Schlichting, H., *Boundary Layer Theory*, McGraw-Hill, New York, 1960, pp. 66-74.
- <sup>2</sup>Floberg, L., "On the Ball Flowmeter and the Ball Viscosimeter," *Acta Polytechnica Scandinavica*, Mechanical Engineering Series No. 36, 1968.
- <sup>3</sup>Happel, J. and Brenner, H., *Low Reynolds Number Hydrodynamics with Special Applications to Particulate Media*, Prentice-Hall, New York, 1965, pp. 298-328.
- <sup>4</sup>Brenner, H. and Happel, J., "Slow Viscous Flow Past a Sphere in a Cylindrical Tube," *Journal of Fluid Mechanics*, Vol. 4, 1958, pp. 195-213.
- <sup>5</sup>McNown, J. S., Lee, H. M., McPherson, M. B., and Engez, S. M., "Influence of Boundary Proximity on the Drag of Spheres," *Proceedings of the Seventh International Congress of Applied Mechanics*, Vol. II, Pt. 1, London, 1948, pp. 17-29.

## Preston Tube Calibration Accuracy

Arild Bertelrud\*

FFA, The Aeronautical Research Institute of Sweden,  
Bromma, Sweden

### Introduction

A large number of methods exists for measuring local skin friction, direct ones using a skin friction bal-

Received May 5, 1975; revision received August 28, 1975. This investigation was sponsored by the Swedish Material Administration of the Armed Forces, Air Material Department.

Index category: Boundary Layers and Convective Heat Transfer-Turbulent.

\*Research Engineer. Member AIAA.

ance, and indirect ones relying on similarity arguments.<sup>1</sup> One of the most common similarity methods is the surface pitot tube in the form suggested by Preston.<sup>2</sup> Over the years several investigations have been carried out to establish a calibration of good accuracy valid in both incompressible and compressible flow. For incompressible flow the calibration by V.C. Patel<sup>3</sup> is frequently used, while differences in the necessary compressibility transformations make it more difficult to establish a "preferred" calibration at high Mach numbers.<sup>4,5</sup>

Common to most of the calibrations is the use of Preston's original calibration variables  $x^*$  and  $y^*$ . These are the logarithms of the nondimensional pressure and skin friction parameters and hence are less suitable for assessing the real measurement accuracy than other variables suggested more recently.<sup>6,7</sup> Patel's calibration<sup>3</sup> is represented by three expressions in  $x^*$  and  $y^*$  that do not match, and to overcome this difficulty different interpolations have been suggested for the regions near joints.

Although Patel's calibration is the one most commonly used, other plausible incompressible expressions exist and the complete data set represent a considerable uncertainty in skin friction. This, together with the difficulties in using Patel's different expressions, led to the present study of Preston tubes in incompressible pipe flow. The main objective, apart from obtaining data for a wide range of diameters and relative lengths, was to investigate the sensitivity of the variables to how the basic measurements are performed. To be more specific: for pipe flow calibration, what is the dependence on where and how the static pressure is measured and on which stations are used to estimate the skin friction?

### Experiments

Details about the experiment and tabulated results are given in Ref. 8. Preston tubes of diameters 0.6 to 19 mm were calibrated in a 105 mm diameter pipe at speeds from 8 to 45 m/sec. A flattened tube of 0.24 mm height was also tested. Five different 19 mm tubes with the relative lengths in the range  $6.7 > L/D > 1.6$  were used. The 19 mm tubes extended outside the logarithmic region, but it should be noted that some of the calibrations used in the literature have been based on Preston tubes of comparable sizes.<sup>9</sup> As a check on the results obtained two different lengths of the 10 mm tubes were also tested.

Checks on flow conditions in the pipe prior to the tests showed that the velocity profile was fully developed turbulent at the measurement station, and the measured friction factor was in agreement with Prandtl's equation for a smooth pipe.<sup>10</sup>

### Results

Figure 1 shows the results obtained from systematic variations of the tube diameter presented in the usual variables  $x^* = \log_{10}(\Delta p D^2 / 4 \rho v^2)$  and  $y^* = \log_{10}(\tau D^2 / 4 \rho v^2)$ . The points in this figure were obtained by using the static pressure farthest from the probe tip (but at the same streamwise position) and the pressure drop downstream of the Preston tubes, as in Patel's calibration. The pressures at these stations were influenced by the presence of the Preston tube by a shift of all the points corresponding to the pressure loss over the Preston tube. The influence of different choices available for measuring static pressures and streamwise pressure drops is illustrated in Fig. 1 by plotting the "uncertainty rectangle" for one measurement. The resulting uncertainty appears to be of equal order of magnitude with the deviation between different curves suggested in the literature. It should be noted that other possible causes for this deviation exist. (One is nonlinearity of the manometers, as pointed out by Preston<sup>11</sup>).

The logarithmic representation tends to obscure real and important differences in the measured quantities, and various

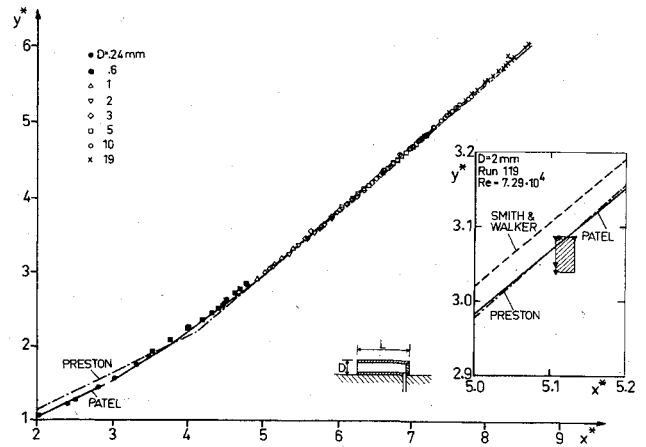


Fig. 1 Results from systematic variations of tube diameter, expressed in  $x^*$ ,  $y^*$  variables. Present data is compared with the curves of (Preston,<sup>2</sup> Patel<sup>3</sup> and Smith & Walker<sup>12</sup>). The "uncertainty rectangle" for one particular measurement is denoted  $\square$  (— Preston<sup>2</sup>, — Patel<sup>3</sup>, — Smith & Walker<sup>12</sup>).

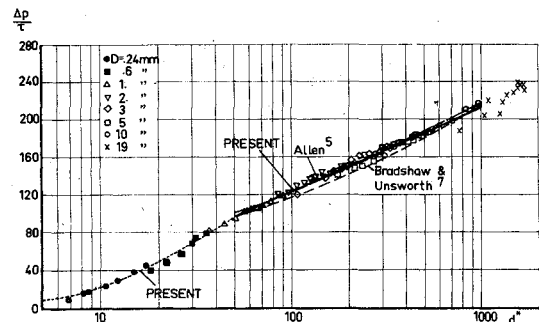


Fig. 2 Present results at speeds lower than 34 m/sec, plotted as  $\Delta p / \tau$  vs  $u_\tau D / \nu$ . .... Present, lower region. — Present (equation) — Allen,<sup>5</sup> — Bradshaw & Unsworth.<sup>7</sup>

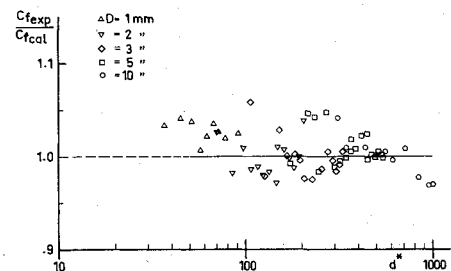


Fig. 3 Ratio of experimental  $C_{f_{exp}}$  through  $C_{f_{cal}}$  deduced from the calibration curve in the region  $50 < d^* < 1000$ .

other parameters have been suggested. One such pair is  $\Delta p / \tau$  and  $d^* = u_\tau D / \nu$ .<sup>6,7</sup> Another possibility,  $\Delta p / \tau$  and  $\Delta p D^2 / \rho v^2$  might be more convenient, but here  $\Delta p / \tau$  and  $d^*$  are used for comparison with Bradshaw and Unsworth.<sup>7</sup>

Figure 2 shows the data plotted in these variables and compared with the calibrations of Bradshaw-Unsworth<sup>7</sup> and Allen<sup>5</sup> reduced to incompressible conditions. Unlike most calibrations which are based on local properties only, the freestream velocity  $U_e$  is used in Allen's expression; for pipe flow  $U_e$  must be replaced by the center-line velocity. Bradshaw-Unsworth's expression is based on an interpolation between two of Patel's curves that do not match, and the slight bend in their curve may be influenced by how the interpolation has been performed. It is noted that the present results fall with reasonable accuracy on a straight line.

Two of the 13 Preston tubes showed deviating behavior above the pipe mean velocity  $\bar{U} = 34$  m/sec, and therefore all data from other tubes above this velocity have also been ex-

cluded from Figs. 2 and 3 and the analytic representations. The 19 mm tubes were furthermore found to have a different type of calibration curve, and they have also been excluded from the analytic representations. The five 19 mm tubes showed no variation in the tested range of relative lengths, and this observation was confirmed by the extra 10 mm tube used. This is not a final proof that there is no dependence at smaller tube diameters, but it is a clear indication.

The results can be represented by the least-squares fit

$$\frac{\Delta p}{\tau} = 87.77 \cdot \log_{10} \left[ \frac{u \tau^D}{\nu} \right] - 51.93 \quad 50 < \frac{u \tau^D}{\nu} < 1000$$

or

$$\frac{\Delta p}{\tau} = 38.85 \cdot \log_{10} \frac{\Delta p D^2}{\rho \nu^2} - 111.92$$

$$2.5 \cdot 10^5 < \frac{\Delta p D^2}{\rho \nu^2} < 2.1 \cdot 10^8$$

It should be observed that reducing the data directly from experimental points expressed as  $\Delta p/\tau$  vs  $d^*$ , gives a different result from curve-fitting  $x^*$ ,  $y^*$  values and then transforming to  $\Delta p/\tau$ ,  $d^*$ .

Figure 3 shows the scatter in estimated  $C_f$  resulting from the scatter in the calibration experiments. The standard deviation in 0.022. For the point illustrated in Fig. 1 with an "uncertainty rectangle", the values obtained are  $C_{f_{exp}}/C_{f_{cal}} = 0.89 - 1.04$ .

The pressure magnitudes were: dynamic pressure based on maximum velocity:  $U_e$  101 N/m<sup>2</sup>; Dynamic pressure based on mean velocity  $\bar{U}$  69 N/m<sup>2</sup>; Preston tube indicated pressure  $\Delta p_e$  34 N/m<sup>2</sup>; and static pressure range 2 N/m<sup>2</sup>.

### Conclusions

The results of the present investigation show that: in terms of  $x^*$ ,  $y^*$  variables the results of Patel are, not unexpectedly, verified. The differences between existing calibration curves fall within an "uncertainty rectangle" for plausible choices on how static pressure and pressure drop measurements can be performed.

Greater accuracy can be obtained with new variables. A calibration based on present data gives straight line fit in wall variables  $\Delta p/u_\tau$  and  $u_\tau D/\nu$ . The relative length is unimportant in the region tested, down to  $L/D = 1.6$ .

### References

- <sup>1</sup>Rechenberg, I., "Messung der turbulenten Wand-schubspannung," *Zeitschrift für Flugwiss.*, Vol. 11, Heft 11, Nov. 1963, pp. 429-438.
- <sup>2</sup>Preston, J.H., "The Determination of Turbulent Skin Friction by Means of Pitot Tubes," *Journal Royal Aeronautical Society*, Vol. 58, Feb. 1954, pp. 109-121.
- <sup>3</sup>Patel, V.C. "Calibration of the Preston Tube and Limitations on its Use in Pressure Gradients," *Journal of Fluid Mechanics*, Vol. 23, Part 1, Sept. 1965, pp. 185-208.
- <sup>4</sup>Hopkins, E.J. and Keener, E.R., "Study of Surface Pitots for Measuring Turbulent Skin Friction at Supersonic Mach Numbers-Adiabatic Wall," NASA TN D-3478, July 1966.
- <sup>5</sup>Allen, J.M., "Evaluation of Preston Tube Calibration Equations in Supersonic Flow," NASA TN D-7190, May 1973. Synopsis in *AIAA Journal*, Vol 11, Nov. 1973, pp. 1461-1462.
- <sup>6</sup>Head, M.R. and Vasanta Ram, V., "Simplified Presentation of Preston Tube Calibration," *Aeronautical Quarterly*, Vol. 22, Part 3, Aug. 1971, pp. 295-300.
- <sup>7</sup>Bradshaw, P. and Unsworth, K., "A Note on Preston Tube Calibrations in Compressible Flow," Imperial College Aero Rept. 73-07, London, 1973.
- <sup>8</sup>Bertelrud, A., "Pipe Flow Calibration of Preston Tubes of Different Diameters and Relative Lengths Including Recommendations on Data Presentation for Best Accuracy," Aeronautical Research Institute of Sweden, Bromma, Sweden, FFA Rept. 125, 1974.

<sup>9</sup>Ozarapoglu, V., "Measurements in Incompressible Turbulent Flows," Doctoral Thesis, University of Laval, Quebec, Canada, Feb. 1973.

<sup>10</sup>Schlichting, H., *Boundary-Layer Theory*, 6th ed., McGraw-Hill, New York, 1968, p. 574.

<sup>11</sup>Private communication.

<sup>12</sup>Smith, D. and Walker, J., "Skin-Friction Measurements in Incompressible Flow," NASA TR R-26, 1959.

## Experimental Investigation of Boron/Lithium Combustion

R. Mestwerdt\* and H. Selzer†

DFVLR Institut für chemische Raketenantriebe  
Standort Trauen, West-Germany

### Introduction

**A**IR augmented rockets offer some advantages for long propelled missions in comparison to conventional rockets. The necessary reduction of the tank-weight and the high heat of combustion favor the use of boron as a fuel. Unfortunately, the complete reaction of boron in air can only be achieved if the ignition temperature is higher than 1950 K, otherwise a dense shielding oxide layer will be formed preventing further fast oxidation.

To overcome these difficulties, several approaches are being studied: a) to control the total reaction process in a way that the boron particles are heated up to 1950 K in a fuel rich environment; b) to modify the reaction process by the formation of different intermediates as for example in the presence of OH-radicals; and c) to treat the boron itself in order to avoid a closed oxide layer.

As the first two approaches are being studied by Schadow<sup>1,2</sup> and Boussios,<sup>3</sup> the third area of investigation will be reported here. From theoretical considerations the system boron/lithium looked very promising.<sup>4,7</sup> Attempts to coat the boron had been not successful in avoiding combustion problems, therefore a binary metal compound was used. Neither the Li/B product could be ordered nor a description found on how to produce it. Thus, the first step was to find a way to produce a co-melt of Li/b.

### Experiments

Figure 1 illustrates the small oven used to produce the compound. About 1.5 g of crystalline boron (purity 98/99%) was placed in a tantalum cylinder together with lithium particles in argon atmosphere. The cell was sealed and heated up to 900 K in vacuum in order to avoid oxidation of the tantalum and to measure the heat of formation of the Li-B compound by the analysis of the temperature/power plot. The molar ratios (Li:B) investigated were between 1:2 and 1:6. After the reaction, the cell contained two different materials: a granular part which was mainly boron, and a hard compact body which consisted of one part lithium and two parts boron. The product LiB<sub>2</sub> is oxidized in air and had to be stored therefore in argon.

To run the tests at temperatures higher than 2000 K an electrical resistance-furnace was selected using a graphite tube. A

Presented as Paper 75-247 at the AIAA 13th Aerospace Sciences Meeting, Pasadena, Calif., January 20-22, 1975; submitted March 7, 1975; revision received May 5, 1975.

Index categories: Fuels and Propellants, Properties of; Combustion in Heterogeneous Media.

\*Phys.-Ing. (grad), Deutsche Forschungs-und Versuchsanstalt für Luft- und Raumfahrt e.V.

†Doctor rerum, naturalium, ERNO Raumfahrt GmbH.